STUDY OF THE CATALYTIC CONVERSION AND ADSORPTION OF ABIETIC ACID ON ACTIVATED CARBON: EFFECT OF SURFACE ACIDITY

RAFAEL GARCÍA,*[a] LORENA PERALTA,[a] CRISTINA SEGURA,[b] CATHERINE SEPÚLVEDA,[a]
I. TYRONE GHAMPSON,[c] NESTOR ESCALONA[c,d]

[a]Universidad de Concepción, Facultad de Ciencias Químicas , Edmundo Larenas 129, Concepción, Chile; Tel:56-0412204324
[b]Universidad de Concepción, Unidad de Desarrollo Tecnológico, Avda. Cordillera 2634, Parque Industrial Coronel, Coronel, Concepción, Chile
[c] Departamento de Ingeniería Química y Bioprocesos, Escuela de Ingeniería, Pontificia Universidad Católica de Chile,
Avenida Vicuña Mackenna 4860, Macul, Santiago, Chile.
[d] Departamento de Química Física, Facultad de Química, Pontificia Universidad Católica de Chile

ABSTRACT

This study reports the adsorption and catalytic conversion of abietic acid as representative compound of tall oil, using activated carbons. Acid functional groups present on CGRAN activated carbons favored the adsorption of abietic acid, probably through a physical adsorption mechanism. In contrast, the conversion of abietic acid was not favored in DARCO activated carbon by increase of acid sites thought HNO_3 treatment. The detection of neoabietic, palustric and/or levopimaric acids as reaction products indicate that the transformation of abietic acid was by dehydrogenation and/or isomerization routes. The negative influence of acid sites on the catalytic activity, in addition to the non-detection of volatile products, suggests that the cracking pathway for the conversion of abietic acid over these catalysts can be ruled out. Contrasting effects of the surface groups on the adsorption capacity and the conversion was observed: strong acid sites of CGRAN activated carbon favor the adsorption of abietic acid and decrease competitive adsorption between substrate and solvent, while conversion is not favored by these acid sites.

Keywords: Activated carbon, abietic acid, tall oil, adsorption capacity.

1- INTRODUCTION

Fossil fuels are considered a fundamental raw material for the development and operation of all countries. The high dependence on these non-renewable resources has been a great concern to politicians, economists, scientists and citizens around the globe. In this context, Maggio and Cacciola[1] estimated that the maximum values in the global production of fossil fuels would be: 30 Gb/year between 2009 and 2021 for oil, 132 Tcf/year between 2024 and 2046 for natural gas, and 4.5 Gtoe/year between 2042 and 2062 for coal. The imminent depletion of fossil resources has sparked the exploration and production of biofuels from biogenic waste such as forest products, sugar cane, sugar beet, sunflower and algaes.[2] The biomass-derived fuels have a low content of sulfur, nitrogen, metals residues, and also contribute to carbon recycling and minimize greenhouse gases emission, which has increased the interest in these renewable resources.[3]

A large amount of black liquor is formed as by-products from the conversion of biomass by the Kraft process. Resin oil or tall oil can subsequently be extracted from black liquor and used as a potential feedstock to obtain third generation bio-fuels[4]. Coll et al.[5]obtained 350 kg of resin acids, 300 kg of fatty acids and 350 kg of distilled resin oil from 1000 kg of crude resin oil fractionation.Resin acidis composed mainly of abietic, dehydroabietic and neoabietic acids. In addition to these products, minor components such as diterpenoids, diterpene alcohols, aldehydes, hydrocarbons and oxygenates compounds can be obtained from tall oil.These compounds have the potential to be feedstock for the production of fuels and chemicals.

Currently, several researches have focused in the use of resin acid as fuel additives or obtention of high values chemicals. In this context, the conversion of tall oil to fuels and chemicals over TK-555 (Ni-Mo), C-424 (Ni-Mo) and C-448 (Co-Mo) commercial catalysts have been reported.[5] The results showed high conversions over all catalysts studied. Moreover, the addition of phosphorus ($AlPO_4$) to the TK-555 catalyst enhanced the cracking activity, probably by presence of Brönsted acid sites.For the three catalysts used some textural properties are summarized, however the possible influences of surface chemistry, mainly acid-base catalysts properties is not discussed.

In the early works, Clark *et al.* studied the cracking of resin oil over SiO_2-Al_2O_3-ZrO_2 catalyst in a fixed bed reactor at atmospheric pressure and 350-500 °C.[6] The highest yield was obtained at 500°C, where the principal products observed were methylcyclopentanes, dimethylcyclopentanes, toluenes, xylenes, diethyl-benzene, 1,3,5-trimethyl benzenes, 1,2,4-trimethyl benzenes, naphthalene, methyl naphthalenes, 2,6-dimethyl naphthalenes and anthracenes. The minor products observed were not obtained by cracking pathway of resin acids conversion, but were attributed to the rearrangement and disproportion

routes from resin acids. This article discusses the effect of operating variables used in the products formation. However, the textural and chemical properties of the catalyst (acid-base) might influence in the distribution of products was not discussed.

The production of high value chemical from catalytic conversion of vegetable oils was reported by Kang and Bathia[7]. These authors studied the effect of acidity and porosity of HZM-5, USY, MCM-41 and SBA-15 commercial catalysts on catalytic cracking of palm oil and vegetable oils in a FCC reactor at 450 °C and 1 bar.The results showed that all the catalysts were active towards gasoline-type products, mainly kerosene and diesel. However, the catalysts were deactivated by coke formation due to the acidity of the solids. Finally they comment that this catalytic process can be improved adequately complementing textural and acid-base properties of the catalysts. In the same line, the catalytic cracking of tree oils over CaO, Al_2O_3 and MCM-41 catalysts at 450 °C had been studied by Junming *et al.*[8] The biofuels obtained showed similar properties to fuels derived from petroleum, demonstred that the acid-base catalysts properties may influence the product distribution obtained.

According to Murzin et al[9], the heterogeneous catalytic transformation as hydrogenation, deoxygenation or isomerization of vegetable based raw materials, has been scarcely studied. These authors reported the catalytic deoxygenation of fatty acid over twenty heterogeneous catalysts using a semi batch reactor at 300 °C of temperature and 6 bar of pressures.The results showed catalytic conversion of fatty acid over all catalysts studied, where activated carbon based catalysts was the most active. However, the chemical characterization of the catalysts related to the acid-base properties associated to the catalytic activity and selectivity, was not reported.

Wang and co-workers, studied the kinetic of the catalytic isomerization of resin acids of tall oil on activated carbon palladium supported catalyst in a batch reactor at 270 °C and 5 bar of N_2 pressure.[10] The catalyst was active for the isomerization, hydrogenation and dehydrogenation reactions of the resin acids presents in the tall oil. The reaction products were neoabietic acid and palustric acid from isomerization of abietic acid, while dehydroabietic acid was obtained through dehydrogenation of abietic acid.It is shown that the isomerization of resin acid can be occurs under nitrogen atmosphere and moderate conditions of temperature and pressure, using activated carbon based catalysts. However, the surface chemistry (acid-base properties) influence of the support was not considered in this study.

The production of biofuels from vegetable oils as alternatives to fuels is summarized in the Haung-Kraft research[11]. These authors show an industrial process for biofuels production, from vegetables oils and/or fat-like feeds, using activated carbon as catalyst in the GREASOLINE® process, developed

and invented by Greasoline GmbH and Fraunhofer UMSICHT in Germany. This process allows the production of airplane-grade biofuel, but such has been indicated previously, the physicochemical characteristics (acid-base properties) of the activated carbon based catalysts are not specified.

Therefore, considering the high production of tall oil as a by-product from the pulp industry, and the potential of activated carbon, the objective of this work was to study the adsorption and conversion of abietic acid as representative compounds of tall oil, using two commercial activated carbons. These activated carbons were modified by different processes to obtain materials with different textural and acidic properties. These properties are correlated to the abietic acid adsorption behaviour and the corresponding catalytic activity.

2. MATERIAL AND METHODS

2.1 Catalysts and modifications

2.1.1 Catalysts

As catalysts, two commercial activated carbons were used, CGRAN and DARCO (obtained from Norit Americas, Inc.). In order to modify their chemical surface two modification treatment methodology were considered.

2.1.2 Thermal modification with helium treatment.

The thermal treatment of CGRAN and DARCO was carried out under He flow from 25 °C up to 1050 °C, at a heating rate of 10°C min^{-1}, and maintained at 1050 °C for 3 h, in order to reduce the surface functional groups concentration. The untreated samples were denoted as CGRAN and DARCO, while the He-treated samples were denoted as CGRAN-He and DARCO-He.

2.1.3 Chemical modification with HNO$_3$ treatment.

1 g of DARCO activated carbon was oxidized with HNO$_3$ (3 and 6 mol L^{-1}) at 80 °C for 1 h following a procedure reported by Aguilar et al.[12]. The samples were then thoroughly washed with water until a neutral pH of the filtrate was obtained, and then dried at 110ºC for 10 h. The samples were denoted as Darco-N3 and Darco-N6 according to the concentration of HNO$_3$ used (3 mol L^{-1} and 6 mol L^{-1}, respectively).

2.2 Characterization of the catalysts

The BET "apparent" specific surface (S_{BET}) and pore volumes of the catalysts were determined from nitrogen adsorption/desorption measurements at 77 K using Micromeritics TriStar II 3020 equipment. Prior to the measurements, the samples were outgassed at 573 K for 2 h. Micropore volume (Vo) was determined by the Dubinin–Radushkevich method while the total pore volume (Vp) was recorded at a relative pressure of 0.99. Mesopore volume (Vm) was obtained from the difference between Vp and Vo.

Temperature-programmed decomposition (TPD) analyses of the activated carbons were carried out under an inert atmosphere at a heating rate of 18 ºC min^{-1} from room temperature to 1050 ºC, and a helium flow of 50 mL min^{-1}. The amounts of evolved gases (CO_2 and CO) were measured by a thermal conductivity detector (TCD) coupled to a non-dispersive infrared device (NDIR).

FT-IR analyses of the supports were performed on a Nicolet Nexus FT-IR in the middle range (4000–400 cm^{-1}) and averaged after 64 scans. The tablets were prepared using KBr as a support in a 1:100 mg proportion of sample to support.

The total acidity measurements of the activated carbon supports and catalysts were obtained by potentiometric titration of a suspension of carbon in acetonitrile with n-butylamine using an Ag/AgCl electrode, following a well-cited method developed by Cid and Pecchi.[13]

2.3 Abietic acid adsorption isotherms.

The adsorption isotherms were carried out using different masses of activated carbons, between 0.1 to 40 mg with 50 ppm under stirring for 1 h at 30, 50 and 70 °C. After reaching the equilibrium time, the samples were centrifuged and the concentrations of AbA were obtained from calibration curve of UV-VIS spectrophotometer at fixed wave length of 242 nm (Perkin Elmer Lambda-40). The isosteric heat of adsorption q$_{ST}$ was calculated by Clausius-Clapeyron equation using equation 1:[14-16]

$$q_{ST} = RT^2\left(\frac{d\ln[AbA]}{dT}\right) \qquad (1)$$

where [AbA] corresponds to the equilibrium concentration. The isosteric heat of adsorption can be calculated from a $ln\ [C]$ versus $1/T$ plot, at the same level of coverage.[17]

2.4. Catalytic tests

The conversion of abietic acid was carried out in an autoclave stainless steel reactor operating in batch mode. The liquid reactant feed, consisted of abietic acid (100 ppm) in decalin (80 mL). Then, approximately 0.100 g of the selected activated carbon catalyst was added. The system was closed and, to avoid any air contamination, N$_2$ was bubbled through the solution for 20 min. Still under atmospheric pressure of N$_2$ the reactor was heated under stirring to the reaction temperature of 300 ºC. When the reaction temperature was reached, the pressure was increase up to 2 MPa, adding more N$_2$; this pressure was kept constant during the course of the experiment. After 5 hours of reaction, the gases evolved were analysed in a Perkin Elmer Clarus 680 gas chromatograph coupled to a GCMS-SQ8T mass spectrometer (MS-GC). Condensed samples from the reaction liquid mixture, were taken periodically during the reaction and analysed in a Perkin Elmer Lambda-40 spectrophotometer. In order to detect other abietanes structures the spectra in the 200 to 320 nm wavelength was recorded. The concentrations were obtained from a calibration curve previously obtained in the spectrophotometer. The AbA conversion was calculated according to equation 2:

$$\text{Conversion (\%)} = \left(\frac{[AbA]_{initial} - [AbA]_{final}}{[AbA]_{initial}}\right) \times 100 \qquad (2)$$

3. RESULTS AND DISCUSSION

3.1 Characterization of catalysts.

The nitrogen adsorption/desorption isotherms at 77 K of the CGRAN, DARCO, CGRAN-He and DARCO-He catalysts are presented in **Fig. 1a**. All the isotherms are classified as Type I, which is characteristic of a microporous material with a high mesoporous contribution, according to the classification of Brunauer, Deming, Deming and Teller (BDDT)[18, 19]. A similar behaviour was exhibited by the DARCO-N3 and DARCO-N6 catalysts, as shown in **Fig. 1b**. The hysteresis loop in the isotherms of all the solids in **Figs. 1a** and **1b** is assigned to a H4-type (in agreement with IUPAC classifications), indicative of the presence of narrow slit pores characteristic of activated carbons.[20]

The textural properties of all the catalysts obtained from the isotherms are summarized in **Table 1**. The data shows that the apparent surface area of CGRAN activated carbon is higher than the DARCO activated carbon. Also CGRAN is mainly microporous, while DARCO presents a nearly identical contribution from micropores and mesopores. Moreover, **Table 1** shows that after thermal treatment with He, there is an across-the-board decrease in the textural parameters of the CGRAN activated carbon: the surface area (S_{BET}), the total pore volume (Vp) and the micropore volume (V_0) of CGRAN-He decreased by 36%, 15% and 30%, respectively, in comparison to CGRAN. On the other hand, the mesopore volume remained unchanged. In fact, the contribution of mesopores to the porous structure increased from 45% to 55%. This result suggests a partial collapse of the micropores of CGRAN activated carbon after He treatment. This behaviour can be explained by coupling of micropore due to rupture of their inner walls. This partial decrease of microporosity in CGRAN-He, generates an increase in mesoporosity, as can be seen in Table 1. This behavior is also consistent with the decrease in mesopores diameter and the increase in the micropores diameter. The Darco activated carbon behaved differently: there was a marginal decrease in S_{BET} (4%) which originated from a 34% decrease in mesopores volume, while the micropore volume remained relatively constant. It is also worth noting, however, that the micropore diameter of both CGRAN and DARCO increased after He-treatment which suggests a collapse of two adjacent micropores. **Table 1** also shows that oxidation treatment with different concentrations of HNO$_3$ did not significantly modify the textural properties of DARCO activated carbon.[21]
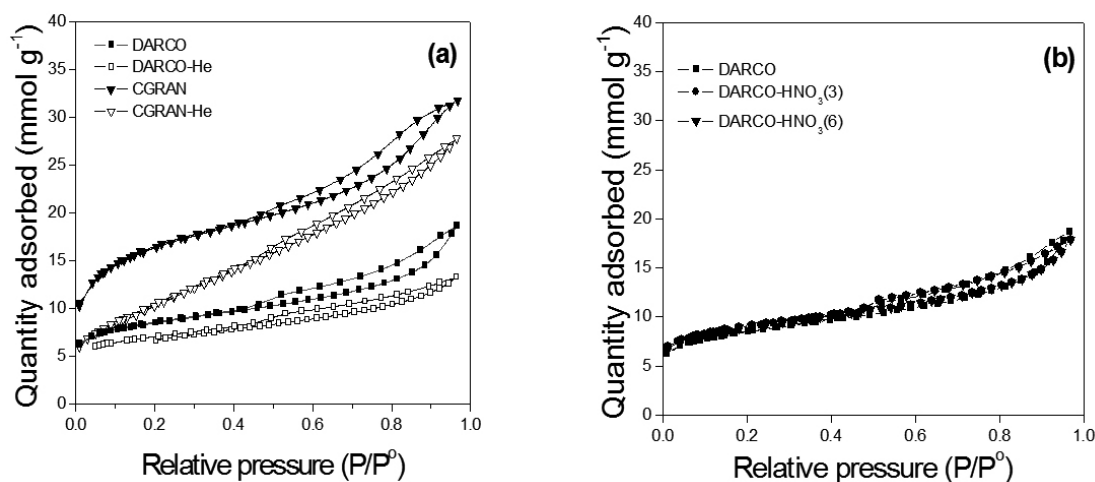
Figures 1: N_2 adsorption–desorption isotherms of (a) DARCO, CGRAN, DARCO-He and CGRAN-He catalysts and (b) DARCO, DARCO-N3 and DARCO-N6 activated carbon catalysts.

Table 1: Textural properties of the catalysts.

Catalysts	S_{BET} (m^2 g^{-1})	V_0 (cm^3 g^{-1})	V_p (cm^3 g^{-1})	V_m (cm^3 g^{-1})	Mesoporous (%)	Mesopore diameter * (nm)	Micropore diameter** (nm)
CGRAN	1340	0.60	1.10	0.49	44	4.1	1.6
CGRAN-He	860	0.42	0.93	0.52	56	3.8	2.7
DARCO	680	0.31	0.65	0.34	52	3.9	2.0
DARCO-He	650	0.30	0.51	0.21	41	3.8	2.7
DARCO-N3	680	0.30	0.53	0.23	43	4.0	2.0
DARCO-N6	700	0.29	0.55	0.26	47	3.9	1.9

* Calculated from N_2 adsorption/desorption isotherms at 77K by BJH method
** Calculated from N_2 adsorption/desorption isotherms at 77K by DFT method

TPD profiles of the activated carbons before and after He and HNO_3 treatments are illustrated in **Fig. 2**. It should be pointed that the scale used to represent the TPD profile of DARCO in Figures 2a and 2b are not the same. The TPD of the CGRAN activated carbon (**Fig. 2a**) displayed a very pronounced peak between 200 and 850ºC, in addition to a lower intense peak centred at 900 °C. Meanwhile, DARCO activated carbon showed two significantly weaker peaks centred at 650°C and 950°C. The effect of He-treatment on the CGRAN and DARCO activated carbons was somewhat similar: the pretreatment completely eliminated the low temperature peak.
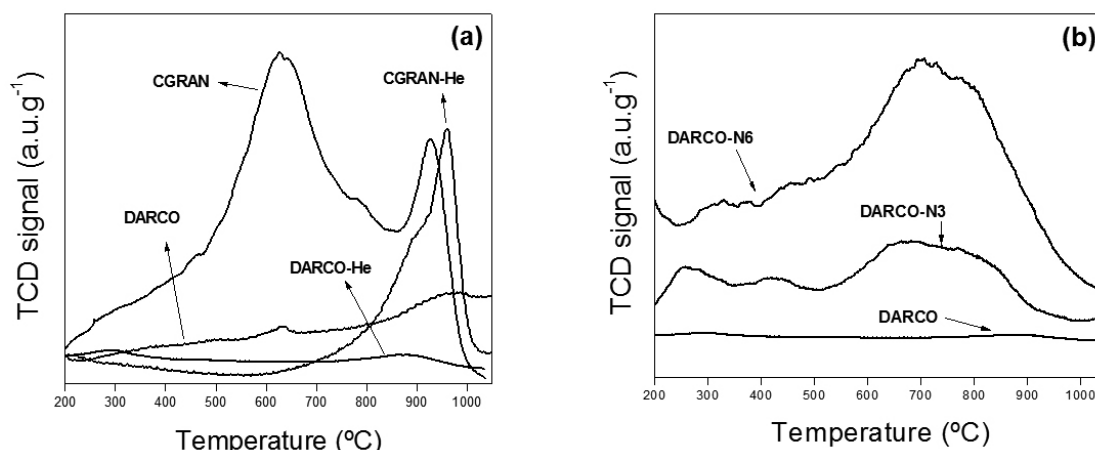
Figures 2: TPD profiles of (a) DARCO, CGRAN, DARCO-He and CGRAN-He and (b) DARCO, DARCO-N3 and DARCO-N6 activated carbon catalysts.

The assignment of surface functional groups according to their gas evolution was supported by NDIR coupled device and the literature.Briefly, carboxylic groups decomposed to carbon dioxide and phenolic or quinonic groups decomposed to carbon monoxide. According to Figueiredo*et al.*[22], the 200-850 °Cpeak observed for CGRAN can be assigned to carboxylic (200 to 250°C), lactones (190 and 650°C), anhydrides (350 to 400°C), phenolics (600 to 700°C), carbonyls (700 to 980°C), ethers (700°C) and quinones (700 to 980°C) acid-type groups. The higher temperature peak centred at 900 ºC for CGRAN and the single peak at 950 °C observed for CGRAN-He catalyst can be attributed to carbonyls (700 to 980°C), ethers (700°C), and quinones (700 to 980°C).Both of these peaks were detected as CO in the NDIR-coupled device.For DARCO the peaks observed can be assigned to carboxylic groups detected as CO_2 by NDIR (200 to 250°C), carbonyl (800 to 900°C) and quinone (700 to 980 °C) groups(detected as CO by NDIR). The very low intense peaks displayed by DARCO-He suggest the near absence of surface functional groups compared to other catalysts.

These results indicate that heat treatment with He on CGRAN catalyst was effective in eliminating or, at the very least, significantly decreasing the amount of surface oxygen functional groups below 850 ºC, while the oxygen groups present above 850ºC were essentially unaffected by this treatment. In relation to DARCO activated carbon, the thermal treatment effectively wiped out the oxygen surface groups in all temperature range.

Figure 2b shows the TPD profiles for DARCO activated carbon and the corresponding samples after nitric acid treatment. DARCO-N3 displayed three broad peaks centred at 250°C, 420°C and 700°C.These first two peaks correspond to CO_2 according to the NDIR analysis, while the third peak corresponds to a mixture of CO and CO_2.A similar profile, but with more intense peaks, was obtained for DARCO-N6. According to Figueiredo*et al.*[22] the peaks obtained for DARCO-N3 and DARCO-N6 can be assigned to carboxylic groups (100 to 400°C), lactone (350 to 400°C), anhydrides (350 to 400°C), phenol (600 to 700°C), ether (700°C), carbonyl (700 to 980°C) and quinonegroups(700 to 980 °C). These results suggest that treatment with HNO_3 over DARCO catalyst created more surface oxygen functional groups by surface oxidation, which becomesmore pronounced with increase in HNO_3 concentration.

The acidity of the activated carbons obtained from potentiometric measurements are summarized in **Table 2**. It shows that CGRAN catalyst displayed higher initial electrode potential (E_0), total acidity and density of acid sites than DARCO catalyst, in agreement with the large amount of oxygen functional groups present on the CGRAN catalyst (deduced fromTPD results). **Table 2** also further illustrates the disparity in the effect of He-treatment between CGRAN and DARCO: the E_0 value decreased considerably after He-treatment of CGRAN while DARCO remained fairly unchanged. The former is consistent with the interpretation from the TPD profile, suggesting the near elimination of acid functional groups (lower temperature peaks) from the surface of CGRAN catalyst.

Table 2: Acid strength (E_0), total acidity and density ofacid sites from potentiometric measurements.

Catalysts	E_0 (mV)	Total acidity (mmol g^{-1})	Acid sites density (mmol m^{-2})
CGRAN	106	1.6	1.2
CGRAN-He	-5	0.6	0.7
DARCO	-15	0.6	0.9
DARCO-He	-12	0.8	1.1
DARCO-N3	60	1.6	2.3
DARCO-N6	91	1.6	2.3

Along the same line, the acidity data for the HNO_3-treated DARCO activated carbon were consistent with the deduction from the TPD profiles: an increase in total acidity and the acid site density is in accordance with the formation of oxygen functional groups on this activated carbon, as illustrated by their respective TPD profiles (**Fig. 2b**).

On the basis of these results, DARCO, DARCO-He and CGRAN-He samples have very weak acid sites with $E_0 < 0$ mV, the DARCO-N3 and DARCO-N6 have strong acid sites with $0 > E_0 > 100$ mV, and CGRAN has very strong acid sites with $E_0 > 100$ mV.[13]The strong acid sites on untreated CGRAN and HNO_3-treated DARCO catalysts can be attributed to the presence of oxygen functional groups.

The FT-IR results (**Figures 3**) of all the catalysts are summarized as follows: CGRAN displayed bands in the 3500–3300 cm^{-1}region assigned to phenolic structures,the 1600–1500 cm^{-1}region attributed to C=O stretching vibrations of lactonic, quinonic or carboxylic groups, and the 1300–900 cm^{-1} region assigned to C–O–C vibrations or C–O stretching of ether, lactonic carboxylic or phenolic groups. Similar but less intense peaks were presented by the CGRAN-He catalyst. DARCO catalyst displayed bands in the same region as DARCO-He; however, the peak for the former was more intense. The 1600–1500 cm^{-1} region is attributed to C=O stretching vibrations of lactonic, quinonic or carboxylic groups, and the 1300–900 cm^{-1} region is assigned to C–O–C vibrations or C–O stretching of ether, lactonic carboxylic or phenolic groups.[21] The FTIR results suggest that heat treatment with He significantly reduces the surface functional groups on the activated carbon, in complete agreement with TPD profiles shown in **Fig. 2a**.
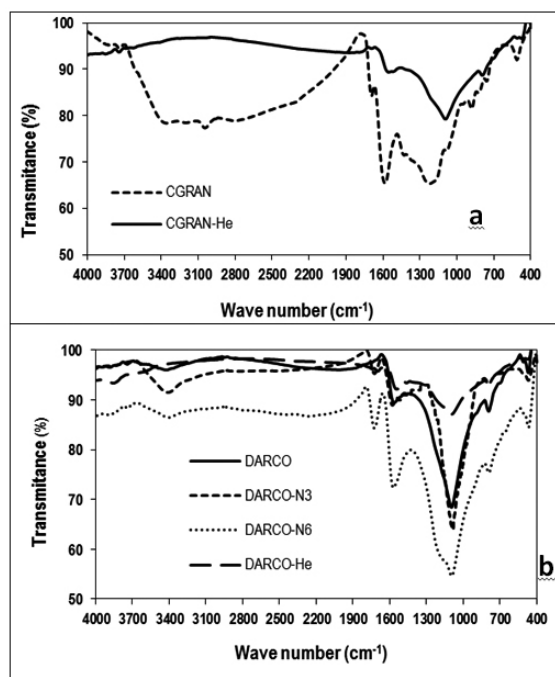
Figures 3: FTIR spectra of activated carbons.

The chemical modification with HNO_3 on DARCO activated carbon intensified the peaks of the FT-IR spectra. DARCO-N6 displayed the highest intensity with peaks in the 3500–3300 cm^{-1} region assigned to phenolic structures, in the 1600–1500 cm^{-1} region attributed to C=O stretching vibrations of lactonic, quinonic or carboxylic groups, and in the 1300–900 cm^{-1} region, assigned to C–O–C vibrations or C–O stretching of ether, lactonic carboxylic or phenolic groups [21]. These results further confirmed that the chemical modification with HNO_3 increased the surface functional groups on the DARCO activated carbon, in agreement with TPD results.[24]

In summary, characterization results revealed a strong correlation between textural (from N_2physisorption) and surface properties (derived from TPD, acidity measurements and FTIR). The near-eradication of some surface oxygen groups on the CGRAN activated carbon after He-treatment could be linked to the significant observed decrease in the surface area. On the other hand, the effect of He-treatment was considerably less severe on the DARCO activated carbon which is consistent with both textural and surface property results. In contrast to the thermal treatment, surface oxidation of DARCO by HNO_3 was effective in increasing the amount of surface groups without an appreciable change in textural properties. It can be inferred from this data that DARCO is more structurally stable than CGRAN.

3.2 Abietic acid adsorption.

The as-received and treated activated carbons were evaluated for the adsorption of abietic acid and the results are illustrated in **Fig. 4**. The figure depicts the adsorption capacity as a function of equilibrium concentration at

three temperatures (30, 50 and 70 ºC) for the pre- and post-treated CGRAN and DARCO activated carbons. From a previous study of the adsorption rates (not shown here), it was determined that the adsorption equilibrium is reached at 30 minutes. According to Giles classification isotherms[25], the CGRAN and CGRAN-He (**Fig. 4a and 4c**) displayed a "L" type isotherms, characteristic of strong affinity between abietic acid and adsorption site. The DARCO (**Fig. 4b**) and DARCO-He (**Fig. 4d**) activated carbons presented an "S" type isotherm, attributed a lower affinity of abietic acid on the adsorption site as a result of competitive adsorption between the solute and the solvent. The isotherms

for the HNO_3-oxidized samples (DARCO-N3 and DARCO-N6) shown in **Fig. 4e and 4f** were a "L" type adsorption isotherm, characteristics of strong affinity between the abietic acid and the solvent.[26, 27] Additionally, DARCO-N3 displayed an isotherm classified as "L2", where the plateau indicates that all available sites on the surface are distributed in a monolayer, and DARCO-N6 showed an isotherm according to the"L1" subgroup, where the plateau is not observed, indicating that the monolayer covered was not reached.[28] This behavior is consistent with the greater amount of surface functional groups displayed by DARCO-N6.
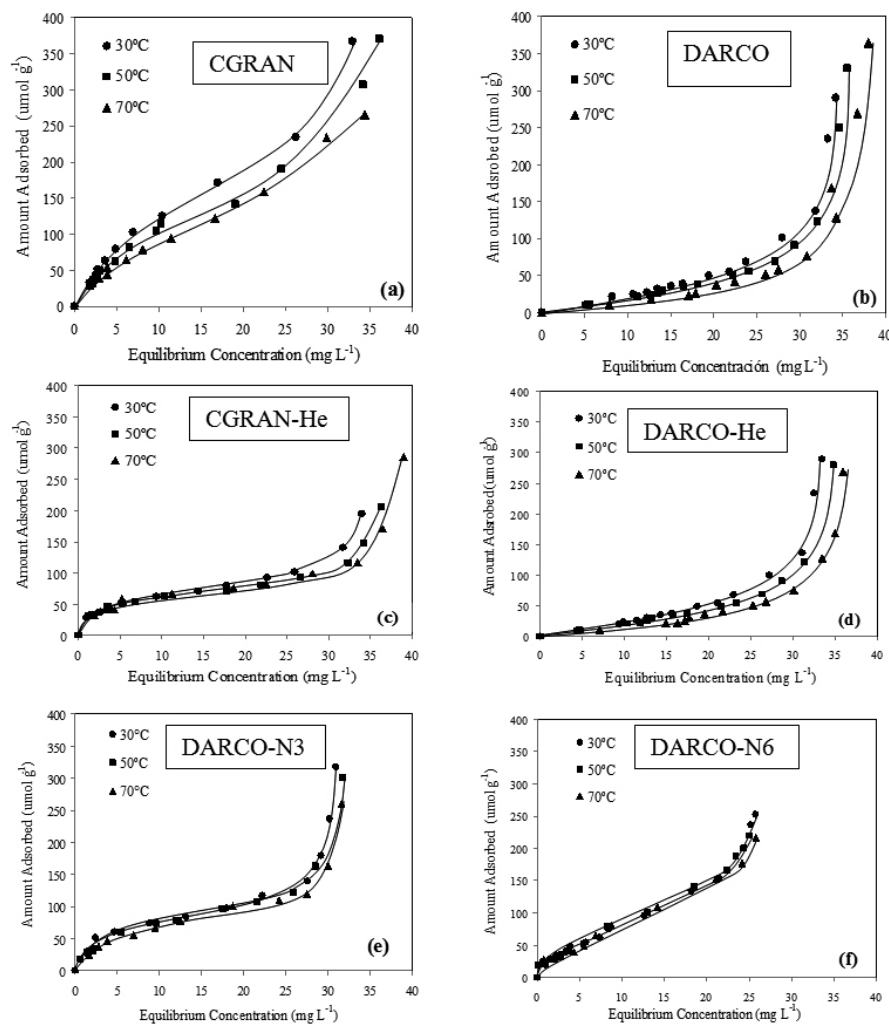
Figures 4: Abietic acid adsorption isotherms of (a) CGRAN and (b) DARCO activated carbon catalysts, (c) CGRAN-He and (d) DARCO-He activated, (e) DARCO-N3 and (f) DARCO-N6.

In regards to the adsorption capacity of activated carbons for abietic acid, **Fig.4a** shows that the adsorption capacity of the CGRAN activated carbon increases with the equilibrium concentration. On the contrary, **Fig. 4b** shows that the adsorption capacity of DARCO slightly increases with the equilibrium concentration up to 30 mg L^{-1}, and then sharply increase after wards at all the three temperatures studied. The results for the as-received activated carbons showed a higher adsorption capacity for CGRAN in comparison to DARCO, which can be attributed to a combination of the higher surface area and the larger amount of oxygen functional groups present on the former.

In order to establish the specific influence of the surface oxygen groups, the adsorption capacity was normalized by S_{BET}.As shown in **Figure 5**, the CGRAN activated carbon has a higher abietic acid adsorption capacity than DARCO activated carbon per surface unity. This greater adsorption capacity of CGRAN was observed at thethree temperatures tested. Depending of the equilibrium concentration CGRAN presents an average of 2-3 times higher

adsorption capacity. However,this difference decreases at higher equilibrium concentration values, due to a greater potential for adsorption.The surface area-normalized adsorption capacity indicates that the presence of oxygen functional groups plays an important role in the adsorption capacity of activated carbons. The higher adsorption capacity of CGRAN could be explained by the presence of strong acid sites (as a result of the higher amount of functional groups), favoring the adsorption of abietic acid up to 30 mg L^{-1}. The converse is true for DARCO.

The effect of He-treatment on the adsorption capacity of abietic acid can be deduced from comparing Fig. 4c to Fig. 4a: the adsorption capacity up to 30 mg L-1 for CGRAN-He was lower than that for CGRAN. On the contrary, the adsorption capacity after He-treatment of DARCO was almost unchanged (Fig. 4b and 4c). These results clearly show a strong dependence of the adsorption capacity on the surface acidity which stems from the presence of surface acid oxygen functional groups. Comparison of the adsorption

capacities of the HNO_3-treated activated carbons accentuates this point: Fig. 5 shows that DARCO-N3 (Fig. 4e) and DARCO-N6 (Fig. 4f) both present higher adsorption capacities compared to DARCO and DARCO-He (Fig. 4b and 4c, respectively). The increase in the amount of oxygen functional groups on activated carbon (carboxylic, lactonic, phenol, anhydride, ether, carbonyl, and quinonic functional groups), as derived from TPD profiles (Fig. 2b) and FTIR measurements, was largely responsible for this behavior due to the inappreciable change in surface area after oxidation (Table 1). These results suggest that the chemical modification of DARCO activated carbon with HNO_3 increases its absorption capacity and affinity for abietic acid due to changes in the nature and amount of surface functional groups.
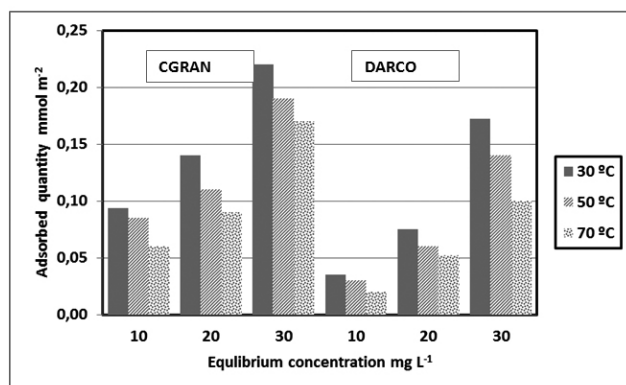

Figure 5: Abietic acid adsorption quantity per area unit, for CGRAN and DARCO activated carbons.

The average isosteric heat of adsorption calculated from ClausiusClapeyron equation (1) were 9 kJ mol^{-1}, 7 kJ mol^{-1}, 6 kJ mol^{-1} and 2 kJ mol^{-1}, for CGRAN, CGRAN-He, DARCO, and DARCO-N6 and DARCO N3, respectively.**Figure 5** also illustrates the relationship between adsorption capacity and temperature: in general, the adsorption capacity is favored at lower adsorption temperatures together with the low values of the isosteric heats of adsorption (less than 10 kJ mol^{-1}), suggesting a physical adsorption mechanism of abietic acid[29]. This behavior is independent on treatment under He, or HNO_3as can be observed by similar trends showed in **Figures4.**

3.3 Catalytic activity

The activity of the activated carbon catalysts were tested in the conversion of abietic acid as a function of time and shown in the Figure 6. This Figure show that DARCO catalyst displayed higher conversion than CGRAN catalyst. **Figure 6** also compares the conversion of the as-received activated carbon catalysts with He-treated counterparts: the CGRAN-He displayed a significantly higher conversion than CGRAN catalyst, a behavior related to the lesser number of surface oxygen groups deduced from TPD, FTIR and acidity results. There was no appreciable difference in the conversion between DARCO and DARCO-He, in agreement with the similarly low amount of surface oxygen groups in both catalysts. Along the same line, the activity of DARCO and the corresponding HNO_3-oxidized samples were compared and shown in **Fig. 6**. The data clearly shows an inverse relationship between conversion and the concentration of HNO_3 used in the modification treatment. The effect of textural properties can be discounted since there were no appreciable changes after the treatment; therefore, this behaviour is clearly an effect of the acid strength and surface oxygenated groups, a testament to the chemical modifications of the surface of DARCO activated carbon, derived from TPD, FTIR and total acidity results. The lowest conversion obtained for DARCO-N6 catalyst can be correlated with their highest acid strength, while the highest conversion exhibited by DARCO was due to their lowest acid strength. These results show that although strong acid sites favour adsorption of abietic acid, they attenuate catalytic activity. These findings also suggest that these sites are not active for catalytic cracking.

In order to corroborate the above assertions, from conversion curves showed in **Fig 6**, the specific rate for the conversion of abietic acid was calculated from the initial slope of conversion vs.time plot, according to the following equation:

$$r_s = \frac{[bxn]}{m} \qquad (3)$$

where r_s is the specific rate (mol g^{-1}h[-1]), b represents the initial slope of the conversion vs. time plot (dimensionless), n is the initial moles of abietic acid (mol), and m is the mass of catalyst (g). The initial intrinsic rate was calculated from the specific rate according to the following equation:

$$r_i = \frac{r_s}{S_g} \qquad (4)$$

where r_i is the initial intrinsic rate and Sg is the surface area of the catalyst. The r_i value represent the moles of abietic acid transformed per surface area of the catalyst perhour(mol m^{-2} h^{-1}). The insets of **Figure 7** show the initial intrinsic rate (i.e. the reaction rate per unit surface area of the solids): Darco was intrinsically more active than CGRAN, suggesting that abietic acid conversion was independent of the textural properties of these catalysts. This opens up the possibility of the surface oxygen groups present on the activated carbons controlling the activity. In fact, CGRAN-He, the solid with the lowest concentration of acidic surface functional groups, displayed the highest catalytic activity. The higher catalytic activity showed by CGRAN-He can be explained by suppression of the surface functional groups (mainly acidic groups) that decomposed during thermal treatment below 850 °C. Due to this decrease of surface acidic functional groups, surface chemistry CGRAN-He has a basic character. In summary, these basic groups, probably carbonyls, ether or quinone types, would be responsible for the higher catalytic activity showed by CGRAN-He.
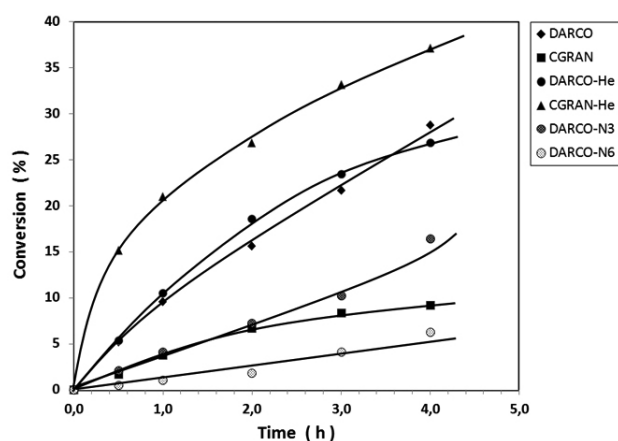

Figure 6: Abietic acid conversion on activated carbon catalysts.

On the other hand, during the abietic acid catalytic conversion assays, volatile products were not detected by GC-MS with a headspace at 200 °C. Also in the UV spectra of the liquid product (not shown here) a new absorbance signal in the range 260 to 280 nm was observed. According to literature references[30, 31], these signals can be attributed to the presence of neoabietic, palustric and/or levopimaric acids,in agreement with reports by other authors.[10, 32] These results indicate that the transformation of abietic acid was by dehydrogenation and/or isomerization routes. This proposed reaction pathway is based on the detection of the compounds mentioned above and also on the negative effect of the acid sites on the abietic acid conversion over these catalysts. Therefore, this behavior, coupled with the non-detection of volatile products by MS-GC, indicates that the conversion of abietic acid did not proceed via the cracking pathway. Finally, it is important to comment that additional work is ongoing in order to optimized reaction products detection and achieved the catalytic essays under hydrogen pressure using metal catalysts supported on activated carbon.

4. CONCLUSIONS

The effect of surface properties of two modified commercial activated carbons on the adsorption and conversion of abietic acid was studied and found to be related to surface oxygen groups which conferred different acid strengths on the carbon. Thermodynamic result suggests that abietic acid adsorption occurs via physical mechanism. The data revealed contrasting effects of the surface groups on the adsorption capacity and the conversion: strong acid sites favor the adsorption of abietic acid and decrease competitive adsorption

between substrate and solvent, while conversion is not favored by these acid sites. The basic chemical surface of CGRAN-He, obtained by thermal elimination of acid surface functional groups in the original material could be favored the dehydrogenation and/or isomerization of abietic acid. In addition, we postulate that, under experimental condition used, abietic acid conversion proceeded via dehydrogenation and/or isomerization pathway.
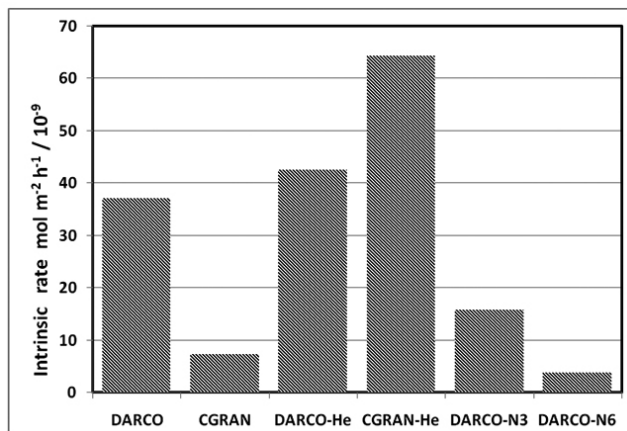

Figure 7: Initial intrinsic rate of the activated carbon catalysts

ACKNOWLEDGEMENTS

REFERENCES

1. Maggio G, and Cacciola G., *Fuel*,**98**, 111–123, (2012)
2. Sanches-Pereira A., Gómez M., *J. Clean. Prod.,***68**, 1-15, (2014).
3. Sharma R. K., Bakshi N. N., *J. Chem. Eng.,***69**, 1071-1081, (1991).
4. Demirbas A., *Fuel*, **90**, 2273-2279, (2011).
5. Coll R., Udas S., Jacoby W.A., *Energy Fuels,***15**, 1166-1172, (2001).
6. Clark I.T., Harris E.E., *J. Am. Chem. Soc.,***74**, 1030-1032, (1952).
7. Kang Y., Bhatia S.,*Energy,***35**, 111-119, (2010).
8. Junming X., Jianchun J., Jie Ch., YunjuanS.,*Bioresour. Technol.,***101**, 5586–5591, (2010).
9. Snare M, Kubickova I, Maeki-Arvela P, Eranen K, Murzin DY.,*Ind. Eng. Chem Res.*, **45**, 5708–5715, (2006).
10. Wang L., Xiaopeng Ch., Jiezhen L., Yueyuan Ch., Xiaodong P., Tong T.,*J. Chem. Eng.*, **152**, 242-250, (2009).
11. Haug P., Kraft A., *ASM Science Journal,***7**, 67-68, (2013).
12. Aguilar C., García R., Soto-Garrido G., Arriagada R., *Top. Catal.*, **33**, 201-206, (2005).
13. Cid R., Pecchi G., *Appl. Catal.,***14**, 15-21, (1985).
14. Poyet S., Charles S.,*Cem. Concr. Res.*, **39**, 1060 –1067, (2009).
15. Liu J., Douglas M., Le Van, *Carbon,***48**, 3454-3462, (2010).
16. Wang G., GrathwohlP.,*Environ. Pollut.*, **175**, 110 – 116, (2013).
17. El-Sharkawy I., Saha B., Koyama S., Srinivasan K,*Int. J. Heat Mass Transfer;***50**, 902-907, (2007).
18. Unger K., *Angew. Chem. Int. Ed.*, **11**, 267-278, (1972).
19. Borislav D., Zdravkov, Čermák J.Jiří, ŠefaraMartin, JankůJosef, *Cent. Eur. J. Chem.,* **5**, 385-395, (2007).
20. Sing, K.S.W., Everett, D.H., Haul, R.A.W., Moscou, L., Pierotti, R.A., Rouquerol, J., and Siemieniewska, T.,*Pure Appl. Chem.,***57**, 603–619, (1985).
21. Moreno-Castilla C., Lopez-Ramon M.V., Carrasco-MarınF.,*Carbon*, 38, 1995-2001, (2000).
22. Figueiredo J., Pereira M., Freitas M., Orfao J., C*arbon,***37**, 1379-1389, (1999).
23. Zielke U., Hüttinger K.J., Hoffman W.P., *Carbon*, **34**, 983-998, (1996).
24. Swiatkowski A., Pakula M., Biniak S., Walczyk M., *Carbon,***42**, 3057-3069, (2004).
25. Giles C., MacEwan T.H., Nakhwa S.N., Smith D., J. Chem. Soc., 3973-3993, (1960).
26. Cabrita I., Ruiz B., Mestre A.S., Fonseca I.M., Carvalho A.P., AniaC.O.,*Chem. Eng. J.,***163**, 249-255, (2010).
27. Baccar R., Blánquez P., Bouzid J., Feki M., Attiya H., SarráM.,*FuelProcess. Technol.,***106**, 408-415, (2013).
28. Limousin G., Gaudet J.P., Charlet L., Szenknect S., Barthe`s V., Krimissa M., *Appl. Geochem.,***22**, 249-275, (2007).
29. Berger A.H., Bhown A. S., *Energy Procedia,***4**, 562-567, (2011).
30. Dell´mour M, Findeisen A, Kalm I, Baatz W and KenndlerE;*The Open Analytical Chemistry Journal*, **2**, 67-73, (2008).
31. Kersten P. J. , Kopper B. J. ,Raffa K. F. and Illman B. L.,*J Chem Ecol.,***32**, 2679–2685, (2006).
32. Souto J. C., Yustos P., Landeros M., García-Ochoa F., *Bioresour. Technol.*, **102**, 3504-3511, (2011).